JCI The Journal of Clinical Investigation

Conditional *Gata2* inactivation results in HSC loss and lymphatic mispatterning

Kim-Chew Lim, … , Masayuki Yamamoto, James Douglas Engel

J Clin Invest. 2012;122(10):3705-3717. https://doi.org/10.1172/JCI61619.

Research Article

The transcription factor GATA-2 plays vital roles in quite diverse developmental programs, including hematopoietic stem cell (HSC) survival and proliferation. We previously identified a vascular endothelial (VE) enhancer that regulates GATA-2 activity in pan-endothelial cells. To more thoroughly define the in vivo regulatory properties of this enhancer, we generated a tamoxifen-inducible Cre transgenic mouse line using the *Gata2* VE enhancer (*Gata2* VECre) and utilized it to temporally direct tissue-specific conditional loss of *Gata2*. Here, we report that *Gata2* VECre–mediated loss of GATA-2 led to anemia, hemorrhage, and eventual death in edematous embryos. We further determined that the etiology of anemia in conditional *Gata2* mutant embryos involved HSC loss in the fetal liver, as demonstrated by in vitro colony-forming and immunophenotypic as well as in vivo long-term competitive repopulation experiments. We further documented that the edema and hemorrhage in conditional *Gata2* mutant embryos were due to defective lymphatic development. Thus, we unexpectedly discovered that in addition to its contribution to endothelial cell development, the VE enhancer also regulates GATA-2 expression in definitive fetal liver and adult BM HSCs, and that GATA-2 function is required for proper lymphatic vascular development during embryogenesis.

Conditional *Gata2* inactivation results in HSC loss and lymphatic mispatterning

Kim-Chew Lim,[1] Tomonori Hosoya,[1] William Brandt,[1] Chia-Jui Ku,[1] Sakie Hosoya-Ohmura,[1] Sally A. Camper,[2] Masayuki Yamamoto,[3] and James Douglas Engel[1]

[1]Department of Cell and Developmental Biology and [2]Department of Human Genetics, University of Michigan Medical School, Ann Arbor, Michigan, USA. [3]Department of Medical Biochemistry, Tohoku University Graduate School of Medicine, Sendai, Japan.

The transcription factor GATA-2 plays vital roles in quite diverse developmental programs, including hematopoietic stem cell (HSC) survival and proliferation. We previously identified a vascular endothelial (VE) enhancer that regulates GATA-2 activity in pan-endothelial cells. To more thoroughly define the in vivo regulatory properties of this enhancer, we generated a tamoxifen-inducible Cre transgenic mouse line using the *Gata2* VE enhancer (*Gata2* VECre) and utilized it to temporally direct tissue-specific conditional loss of *Gata2*. Here, we report that *Gata2* VECre–mediated loss of GATA-2 led to anemia, hemorrhage, and eventual death in edematous embryos. We further determined that the etiology of anemia in conditional *Gata2* mutant embryos involved HSC loss in the fetal liver, as demonstrated by in vitro colony-forming and immunophenotypic as well as in vivo long-term competitive repopulation experiments. We further documented that the edema and hemorrhage in conditional *Gata2* mutant embryos were due to defective lymphatic development. Thus, we unexpectedly discovered that in addition to its contribution to endothelial cell development, the VE enhancer also regulates GATA-2 expression in definitive fetal liver and adult BM HSCs, and that GATA-2 function is required for proper lymphatic vascular development during embryogenesis.

Introduction

GATA factors belong to an evolutionarily conserved family of C4 zinc finger transcription factors that play demonstrably crucial roles in quite diverse developmental programs, including hematopoietic, urogenital, otic, and neuronal developmental elaboration (1–11). GATA-2 was first demonstrated to be essential for hematopoiesis, as *Gata2* homozygous null mutant (*Gata2*$^{-/-}$) embryos die at E10.5 during embryogenesis due to a failure in initial blood cell generation (2). Analyses of null mutant embryonic stem cells and their contribution to in vitro differentiation or to definitive hematopoiesis in reconstituted chimeras supported the argument that GATA-2 is required for the proliferation and/or survival of hematopoietic stem cells (HSCs) (12). Recently, it was shown that *Gata2* haploinsufficiency resulted in altered integrity of the definitive HSC compartment, leading to a reduction in the number of HSCs by essentially one-half (13, 14).

We previously identified and characterized a *Gata2* intron 4 enhancer that conferred reporter gene activity in transgenic mice in both blood and lymphatic endothelial cells (LECs) as well as in poorly characterized subsets of hematopoietic cells (5). Here, we report the generation of conditionally inducible *Gata2* vascular endothelial (VE) enhancer–regulated Cre transgenic lines and the consequences of their induced activity in a floxed *Gata2 (Gata2*^{fl}*)* genetic background. To circumvent the normal E10.5 demise encountered in *Gata2*$^{-/-}$ embryos, we utilized a version of Cre recombinase fused to a tamoxifen-sensitive (Tx-sensitive) ligand-binding domain of the estrogen receptor (CreERT^2, ref. 15). This strategy allowed us to administer Tx, thereby activating Cre and inactivating the *Gata2*^{fl} allele, after the time when embryos would normally encounter the first lethal block in primitive erythropoiesis. Analyses of Tx-treated doubly transgenic *Gata2* compound mutant (Tg^{VE}:*Gata2*$^{-/fl}$) embryos revealed that the VE enhancer harbors what we believe to be a previously undiscovered *Gata2* transcriptional regulatory activity in definitive (fetal and adult) HSCs, and unexpectedly that GATA-2 deficiency in the endothelial lineage results in edema and hemorrhage, leading to late gestational lethality. Histological examination of Tx-treated Tg^{VE}:*Gata2*$^{-/fl}$ embryos revealed blood pooling in the lymphatic vasculature due to failed lymphatic-venous abscission. Thus, these data show that the *Gata2*-null mutant animals that survive the initial primitive erythroid embryonic lethal deficiency normally encountered at E10.5 subsequently die of LEC deficiency at E16.5, thus providing the first evidence to our knowledge that GATA-2 is required for an essential endothelial (either autonomous or non-autonomous) function.

Recently, several groups reported that human patients with *GATA2* mutations presented symptoms of primary lymphedema (16–18), underscoring the vital role of transcription factor GATA-2 in lymphatic development. Through analysis of the conditionally mutant *Gata2* mice described here, we hope to further elucidate the role of GATA-2 in lymphangiogenesis.

Results

Generation of Gata2 VE enhancer–regulated mCherry/CreERT^2 transgenic lines. We generated transgenic mice bearing integrated copies of the VECreERT^2 transgene in which the *Gata2* VE enhancer independently directed the transcription of an inducible Cre recombinase or the fluorescent mCherry (mCh) reporter gene (Figure 1A and ref. 19). Of the transgenic founder animals that were determined by PCR to harbor both transgenes (11 of 44; hereafter referred to as Tg^{VE}), some (7 of 11) stably transmitted both. Their progeny (F_2–F_5 generations) were used for Cre transgene copy number (and other, see below) analyses, and they ranged from 5 to 47 (using *actin* as a normalization control) (ref. 20 and Figure 1B).

When we examined the expression of the co-integrated transgenes, we found that robust mCh epifluorescence in an endo-

Conflict of interest: The authors have declared that no conflict of interest exists.
Citation for this article: *J Clin Invest.* 2012;122(10):3705–3717. doi:10.1172/JCI61619.

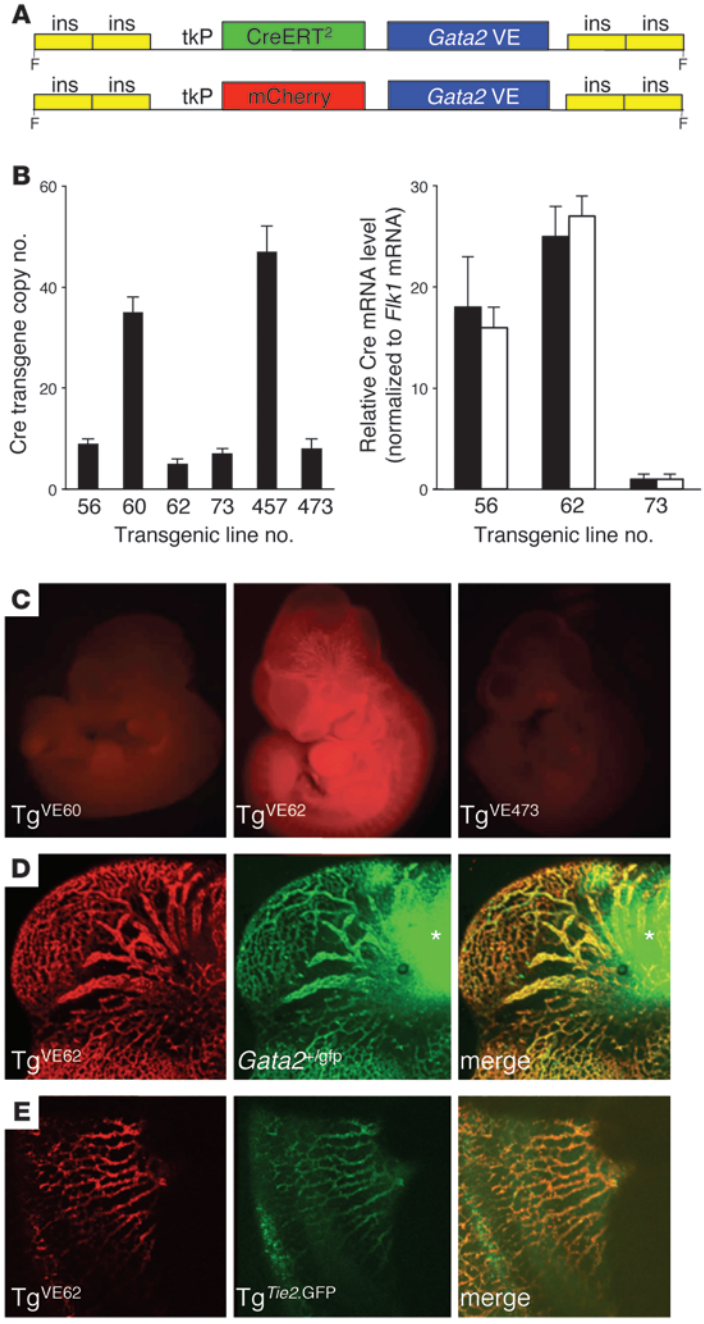

Figure 1

A *Gata2* vascular enhancer confers CreERT^2 and mCh transgene expression in the embryonic vasculature. (**A**) Schematic depicting the CreERT^2 (15) or mCh (19) cDNA driven by the HSV TK promoter (tkP) and the 1.2-kbp *Gata2* VE (5) in VECreERT^2 or VEmCherry expression plasmid, respectively. Each minigene cassette was flanked by tandem repeats of chicken HS4 insulators (ins) (53). Both inserts were excised from the vector and coinjected (1:1) into the pronuclei of mouse oocytes to generate doubly transgenic (Tg^{VE}) mice. F_2–F_5 progeny were used in subsequent analyses (**B**–**E**). (**B**) Cre transgene copy number (normalized to *Actin*) was determined by qPCR to range between 5 and 47 copies. Cre mRNA level (normalized to endogenous endothelia-restricted *Flk1* mRNA) in the heart (black bars) and kidney (white bars) of neonatal Tg^{VE} pups (n = 3 to 8) was determined by RT-qPCR. Of the 3 Tg^{VE} lines that showed significant endothelial mCh staining (see below), Tg^{VE56} and Tg^{VE62} both robustly expressed Cre mRNA, while Cre transcripts were barely detectable in Tg^{VE73}. qPCR primer sequences are listed in Supplemental Table 1. Data represent mean ± SD. (**C**) mCh epifluorescence in representative E10.5 embryos. Of 7 lines that stably transmitted both transgenes, Tg^{VE62} expressed mCh most robustly in an endothelia-specific manner, while in some lines mCh was weakly expressed (e.g., Tg^{VE60} and Tg^{VE473}). (**D**) Coincident expression (merge) of mCh (Tg^{VE62}) and eGFP (generated from *Gata2*$^{+/gfp}$; ref. 21) in the major and fine cranial vasculature in an E10.5 Tg^{VE62}:*Gata2*$^{+/gfp}$ compound mutant embryo. mCh expression temporally and spatially parallels that of eGFP (*Gata2*) in the vasculature. The asterisk indicates a GFP-exclusive area of *Gata2* expression in the ventral midbrain. (**E**) Coincidence (merge) of mCh (Tg^{VE62}) and eGFP (from Tg$^{Tie2.gfp}$) epifluorescence in the major and intersomitic vasculature of an E10.5 Tg^{VE62}:Tg$^{Tie2.gfp}$ embryo, underscoring the vascular endothelial tissue specificity of the Tg^{VE} transgene.

thelia-restricted pattern was detected in E10.5 embryos from 3 lines (56, 62, and 73), while other lines (60, 457, and 473) exhibited no or only very faint vascular mCh fluorescence (Figure 1C and data not shown). Furthermore, in the 3 lines that displayed robust mCh staining, Cre mRNA (normalized to *Flk1* mRNA) in the vascularized heart and kidneys of P0–P2 transgenic pups was easily detectable by RT-qPCR in Tg^{VE56} and Tg^{VE62} but not in Tg^{VE73} mice (Figure 1B). Therefore, only Tg^{VE56} and Tg^{VE62} lines were used for subsequent studies.

To determine whether the vascular expression pattern of the mCh reporter gene reflected genuine GATA-2 expression, we bred Tg^{VE62} to a *Gata2*-eGFP knock-in mouse (21). As depicted in Figure 1D, coincident mCh transgenic expression precisely reflected eGFP fluorescence produced from the endogenous *Gata2* locus, while eGFP alone was additionally (and exclusively) expressed in a cluster of deep ventral midbrain neurons that could be visualized in the same fields (22, 23). Finally, we asked whether mCh fluorescence matched the tissue specificity of a known vascular endothelia-specific gene, the *Tie2* tyrosine kinase (24). As shown in Figure 1E, the transgenic mCh expression pattern in endothelial cells was indistinguishable from that of GFP directed by the *Tie2* gene promoter and enhancer (24) in the intersomitic vasculature.

We further investigated the inducibility and tissue specificity of CreERT^2 activity in these two lines by examining transgene activity in the *ROSA26* reporter *R26R* strain, in which the *lacZ* gene, flanked by transcriptional termination sites and *loxP*

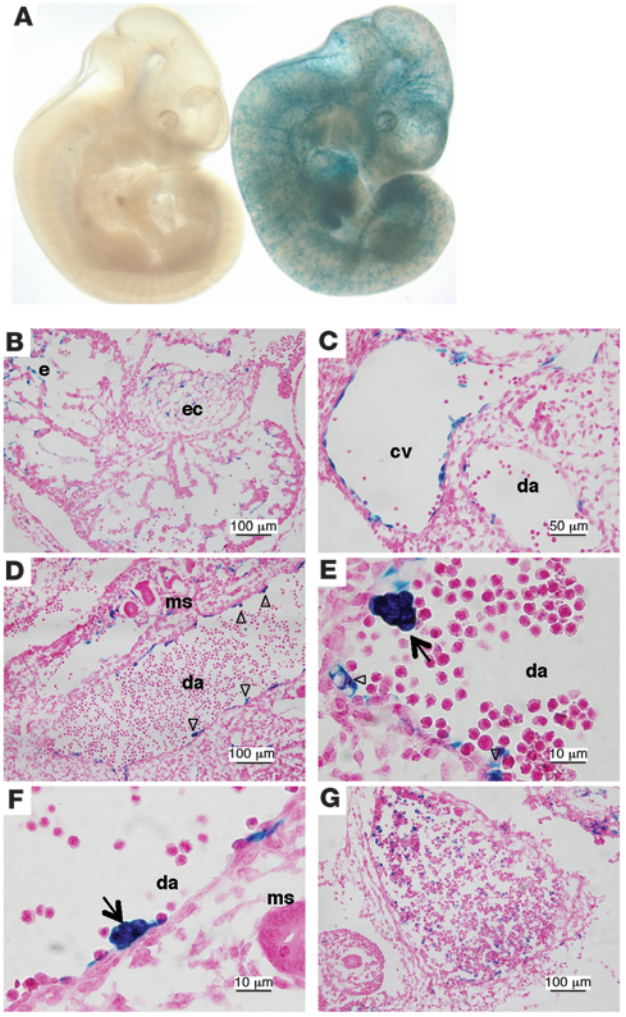

Figure 2
ROSA26R-derived β-gal expression in Tx-treated Tg^{VE} embryos. (**A**) X-gal accumulation is evident in the vasculature of a Tx-treated whole-mount E11.5 Tg^{VE62}:*R26R* compound mutant embryo (right), but not in a (Tx-treated) *R26R* littermate that lacks the Cre transgene (left). In this experiment, embryos were administered Tx from E9 to E11 by gavage of pregnant dams. (**B**–**G**) The Tg^{VE62}:*R26R* compound mutant embryo (**A**, right) was sectioned to further analyze X-gal localization at the cellular level. (**B**) The endocardium (e) and the endocardial cushion (ec) in the E11.5 heart were positive for β-gal activity. (**C**) X-gal staining is also evident in the cardinal vein (cv), from which the lymphatic vascular system develops. (**D**–**F**) Transverse cryosections in the vicinity of the dorsal aorta (da) revealed budding single (arrowheads, **D** and **E**) and clustered (arrows, enlarged view, **E** and **F**) lacZ-positive (rounded) hematopoietic cells. ms, mesonephros. (**G**) Punctate, single-cell X-gal staining was also present in FL endothelial and hematopoietic cells. Scale bars: 1 mm (**A**); 100 μm (**B**, **D** and **G**); 50 μm (**C**); 10 μm (**E** and **F**).

sequences, is integrated at the *ROSA26* locus (25). In this configuration, Cre recombinase activity is reported by β-gal expression only in those tissues in which Cre becomes activated. Without Tx, we could detect no X-gal staining in the doubly transgenic Tg^{VE}:*R26R* embryo or a littermate *R26R* embryo (Supplemental Figure 1A; supplemental material available online with this article; doi:10.1172/JCI61619DS1). However, RT-qPCR analyses of total RNA isolated from their respective yolk sacs confirmed that Cre (as well as mCh, normalized to *Flk1* mRNA) was expressed only in the doubly transgenic Tg^{VE}:*R26R* embryo but not in its littermate *R26R* embryo (Supplemental Figure 1B). In the presence of Tx (administered by daily gavage of pregnant dams from E9 to E11 during embryogenesis), the Tg^{VE}:*R26R* embryo, unlike its control *R26R* sibling (Figure 2A), displayed strong X-gal staining in the blood vasculature, mirroring mCh expression (Figure 1C). Thus, we concluded that the Cre activity in Tg^{VE} is stringently ligand dependent and is functionally expressed in a tissue-specific manner, as anticipated.

When we examined transverse sections of the E11.5 Tg^{VE}:*R26R* embryo (Figure 2A), X-gal accumulation was observed in the endocardium and the endocardial cushions of the developing heart (Figure 2B), as well as in the cardinal vein (Figure 2C), from which a subset of endothelial cells first gain competence to become LECs as they begin to express Prox1 at E9.5 of embryogenesis (26). LECs then delaminate and migrate dorsolaterally to eventually give rise to the first bona fide lymphatic structure, the jugular lymph sac. Further remodeling and elaboration of the embryonic lymph sacs eventually give rise to the mature lymphatic vascular system that is responsible for modulating fluid homeostasis (27).

More interestingly, X-gal–stained individual rounded cells that appeared to be budding from distended endothelial cells into the lumen of the dorsal aorta were routinely observed (Figure 2, D and E, arrowheads) and also appeared in clusters (Figure 2, E and F, arrows). When we examined serial transverse sections along the anteroposterior length of Tx-treated Tg^{VE}:*R26R* embryos (n = 3; >80 serial sections per embryo), we found that 70% ± 6% of hematopoietic clusters stained with X-gal. Such rounded cells budding into the dorsal aorta at this stage have been reported to include HSCs (28, 29). Within the fetal liver (FL), which is the major hematopoietic organ during mid-embryogenesis, we also observed discrete cells displaying β-gal activity (Figure 2G). We were able to validate the previous characterization of the *Gata2* VE element as a vascular endothelial enhancer (5) using this independent strategy, while at the same time discovering that the enhancer might also bear very early hematopoietic lineage specificity.

VE-regulated Gata2 loss in the FL results in depletion of definitive HSCs. To functionally assess the activity of the VE enhancer, we bred the $CreERT^2$ lines in order to conditionally ablate the floxed *Gata2* (*Gata2*^{fl}) allele by removing its fifth exon, which encodes the primary DNA-binding zinc finger (10). In the absence of Tx administration, progeny from these intercrosses were recovered in a normal Mendelian distribution. In particular, *Gata2*$^{-/fl}$ and Tg^{VE}:*Gata2*$^{-/fl}$ sibling animals from litters that were not exposed to Tx were healthy and lived a normal life span. In order to avoid purported effects of Tx administration or Cre expression on embryonic survivability, we tested the progeny of 15 litters from Tg^{VE}:*Gata2*$^{+/-}$ × *Gata2*$^{+/fl}$ intercrosses, with and without different concentrations of Tx, to determine: (a) whether the Cre (or theoretically, the mCh) transgene "poisoned" normal Mendelian survival among the progeny; and (b) the precise dosage of Tx and method of administration that led to robust Cre activation accompanied by no (unusual) embryonic death. Since constitutive loss of GATA-2 results in early embryonic lethality at about E10.5 from a failure to properly execute primitive hematopoiesis (2, 3), Tx was administered after primitive hematopoiesis (beginning between E7 and E7.5) was

Table 1
Distribution of embryos from *Gata2*$^{+/fl}$ × Tg^{VE}:*Gata2*$^{+/-}$ intercrosses

Embryos[A]	+/+	Tg:+/+	+/–	Tg:+/–	+/fl	Tg:+/fl	–/fl	Tg:–/fl
E13.5	6	3	3	2	2	3	7	2
E14.5	4	2	5	7	4	6	5	4
E15.5	2	3	4	2	3	2	3	5
Total	12	8	12	11	9	11	15	11
Observed (%)	13.4	9.0	13.4	12.4	10.1	12.4	16.9	12.4
Expected (%)	12.5	12.5	12.5	12.5	12.5	12.5	12.5	12.5

[A]Pregnant dams were gavaged daily with Tx (0.07 mg/g maternal body weight) from E9 to E11 during embryogenesis. Embryos were collected at the indicated gestational day. Genomic DNAs isolated from yolk sac were used for genotyping by PCR using primers listed in Supplemental Table 1. *Gata2*$^{+/+}$, +/+; *Gata2*$^{+/fl}$, +/fl; *Gata2*$^{+/-}$, +/–; *Gata2*$^{-/fl}$, –/fl; Tg^{VE}:*Gata2*$^{+/+}$, Tg:+/+; Tg^{VE}:*Gata2*$^{+/fl}$, Tg:+/fl; Tg^{VE}:*Gata2*$^{+/-}$, Tg:+/–; Tg^{VE}:*Gata2*$^{-/fl}$, Tg:–/fl.

already in process. Tx was administered to pregnant dams from *Gata2*$^{+/fl}$ × Tg^{VE}:*Gata2*$^{+/-}$ intercrosses beginning on E9 for 3 consecutive days by oral gavage. (Previous studies showed that when Tx was administered to pregnant dams, there was a lag time of 12 hours before levels peaked in the serum of treated animals [ref. 30].) We finally employed an experimentally determined optimal Tx dose of 0.07 mg/g maternal body weight.

Of 89 Tx-treated embryos recovered from 10 litters that were analyzed between gestational days 13.5 and 15.5, Tg^{VE}:*Gata2*$^{-/fl}$ embryos were recovered at the anticipated Mendelian ratios (Table 1). However, we noticed that compared with their littermates, Tx-treated Tg^{VE}:*Gata2*$^{-/fl}$ embryos and yolk sacs appeared to be anemic, with death occurring by E16.5 (see below). We were curious to determine whether the observed pale appearance of the Tx-treated Tg^{VE}:*Gata2*$^{-/fl}$ embryos might be attributable to disruption of a function for GATA-2 in erythropoiesis, since Grass et al (31) independently identified the same *Gata2* enhancer and reported that the VE element was able to potentiate reporter gene expression in transfected murine erythroleukemia cells. Alternatively, the VE enhancer could regulate *Gata2* transcription at some very early stage of hematopoiesis. Our earlier observations, of rounded X-gal–stained cells apparently budding from the dorsal aorta (Figure 2, D–F), lend credence to the latter hypothesis.

To delve more deeply into the etiology of the observed anemia in these embryos, we examined Tx-treated FL cells from E14.5 embryos in triplicate in colony-forming assays in order to determine their ability to generate CFU of either erythroid (burst-forming unit–erythroid [BFU-E]), myeloid (granulocytic, macrophage, or both [CFU-G, CFU-M, or CFU-GM]), or mixed (CFU-GEMM) lineages. Compared with Tx-treated E14.5 wild-type control embryos (*Gata2*$^{+/+}$ with or without Tg^{VE}, n = 11), the total FL cell number in Tx-treated heterozygotes (*Gata2*$^{+/-}$, Tg^{VE}:*Gata2*$^{+/fl}$, n = 13) and Tg^{VE}:*Gata2*$^{-/fl}$ embryos (n = 6) was correspondingly reduced with increasing allelic loss of GATA-2 (Figure 3A). In the latter group of embryos, total FL cell number was reduced to 19% of that in wild-type embryos.

FL cells from these Tx-treated embryos were then seeded into methylcellulose medium supplemented with growth factors

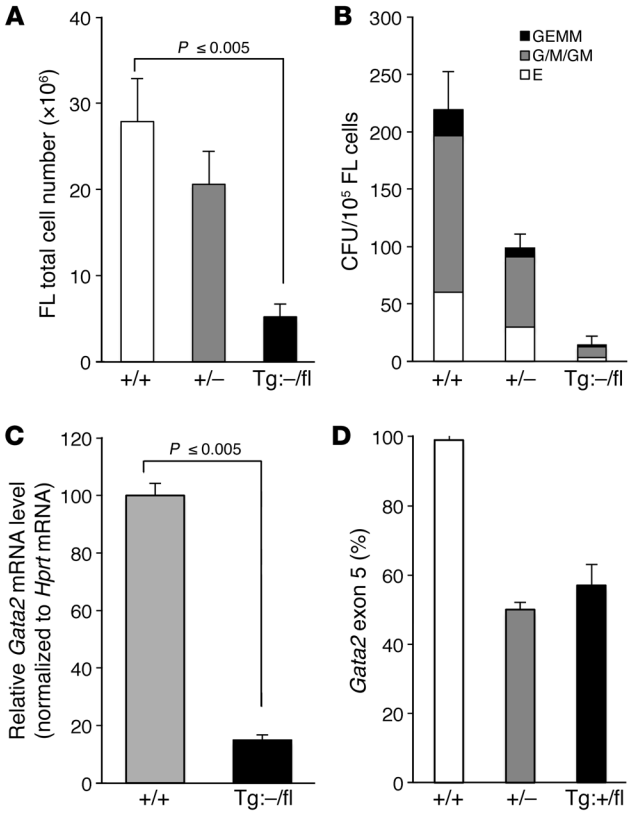

Figure 3
Tx-treated Tg^{VE}:*Gata2*$^{-/fl}$ FL cells fail to generate hematopoietic colonies in vitro. (**A**–**D**) FLs recovered from Tx-treated (see Methods) E14.5 embryos were dissociated into single cells. The total FL cell number in *Gata2* heterozygous (*Gata2*$^{+/-}$, Tg^{VE}:*Gata2*$^{+/fl}$ [+/–]; n = 13) and Tg^{VE}:*Gata2*$^{-/fl}$ embryos (Tg:–/fl; n = 6) was significantly and correspondingly reduced with increasing loss of GATA-2 activity compared with wild-type embryos (*Gata2*$^{+/+}$, Tg:*Gata2*$^{+/+}$ [+/+]; n = 11). (**B**) Total FL cells from the embryos shown in **A** were seeded into methylcellulose medium (M3434). For control embryos, 2 × 10^4 total FL cells were seeded per plate. For Tg^{VE}:*Gata2*$^{-/fl}$ embryos, cells were seeded at multiple concentrations (2 × 10^4, 5 × 10^4, and 1 × 10^5 per plate) in triplicate. Colonies were assessed after 7–12 days in culture. Results represent mean ± SD of 4 independent experiments. Colony numbers were normalized to 10^5 FL cells for graphical illustration. Compared with wild-type FL cells, *Gata2* heterozygous and Tg^{VE}:*Gata2*$^{-/fl}$ cells generated fewer and no CFU colonies, respectively. (**C**) Total RNA was prepared from FL cells of Tx-treated embryos (E9–E11; see **A**) and then quantified (in triplicate) for *Gata2* mRNA (normalized to endogenous *Hprt* mRNA) by RT-qPCR. *Gata2* mRNA was reduced by 85% in Tx-treated Tg^{VE}:*Gata2*$^{-/fl}$ (Tg:–/fl; n = 6) compared with wild-type embryos (*Gata2*$^{+/+}$ [+/+]; n = 6). qPCR primer sequences are listed in Supplemental Table 1. (**D**) Individual hematopoietic colonies (n = 35) isolated from methylcellulose cultures seeded with Tx-treated FL cells from different Tg^{VE}:*Gata2*$^{+/fl}$ embryos from separate experiments (see **B**) were used for genomic DNA extraction, and then qPCR (in triplicate) was performed using primers that detected *Gata2* exon 5 and *Actin* (normalization control; see Supplemental Table 1). *Gata2* wild-type (arbitrarily set at 100%) and heterozygous genomic DNAs from tail snips of adult mice were included to validate the assay. Overall, in Tg^{VE}:*Gata2*$^{+/fl}$ cells, 84% of the single *Gata2* floxed allele was successfully deleted by Tx-induced Cre recombinase. Data represent mean ± SD

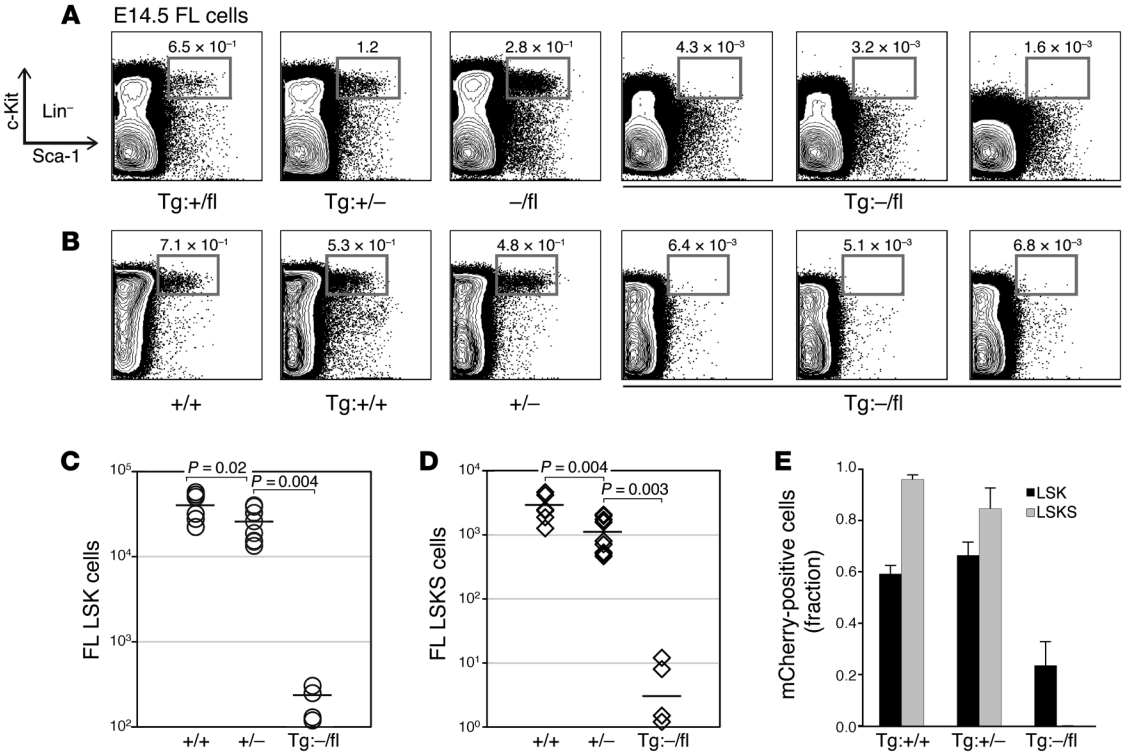

Figure 4

Reduced HSC numbers in Tx-treated Tg^{VE}:*Gata2*$^{-/fl}$ FLs. FLs recovered from E14.5 embryos that had been exposed to Tx in utero were mechanically disrupted, individually processed, and stained with various antibodies prior to analysis by flow cytometry. (**A** and **B**) Representative contour plots for the LSK fraction of 3 Tx-treated *Gata2* control (Tg^{VE}:*Gata2*$^{+/fl}$, Tg^{VE}:*Gata2*$^{+/-}$, and *Gata2*$^{-/fl}$ in **A**; *Gata2*$^{+/+}$, Tg^{VE}:*Gata2*$^{+/+}$, and *Gata2*$^{-/+}$ in **B**) and 3 Tx-treated compound mutant Tg^{VE}:*Gata2*$^{-/fl}$ embryos, which were administered Tx in utero on E9–E11 (**A**) or E11–E13 (**B**). The fraction of LSK cells in the gated areas used to quantify the HSC compartment (boxed) is shown. LSK cells were essentially absent in the Tx-treated Tg^{VE}:*Gata2*$^{-/fl}$ FLs whether Cre was induced during or after the initiation of definitive hematopoiesis. The total number of LSK (**C**) and LSKS (LSK Slam or LSKCD150^{+}CD48^{-}; **D**) cells recovered from the livers of E14.5 embryos, which had been exposed to Tx from E9 to E11, of various *Gata2* genotypes are represented (the ordinate axis is on log scale). *Gata2* wild-type and pseudo-wild-type (*Gata2*$^{+/+}$, Tg^{VE}:*Gata2*$^{+/+}$, *Gata2*$^{+/fl}$ [+/+]; $n = 6$), *Gata2* heterozygous (*Gata2*$^{-/fl}$, Tg^{VE}:*Gata2*$^{+/-}$, Tg^{VE}:*Gata2*$^{+/fl}$ [+/–]; $n = 9$), and Tg^{VE}:*Gata2*$^{-/fl}$ (Tg:–/fl; $n = 4$). Data were compiled from two independent experiments; horizontal black bars represent the mean number of LSK (**C**) or LSKS (**D**) cells of each group of embryos. Statistical significance was determined by Student's *t* test. (**E**) Prominent mCh expression in FL LSK and LSKS cells. FL cells from Tx-treated (from E9 to E11) E14.5 embryos were analyzed for mCh expression by flow cytometry. A large fraction of E14.5 FL LSK or LSKS cells express mCh in Tg^{VE}-positive *Gata2* wild-type (Tg:+/+; $n = 2$) as well as Tg^{VE}-positive *Gata2* heterozygous (Tg^{VE}:*Gata2*$^{+/-}$, Tg^{VE}:*Gata2*$^{+/fl}$ [Tg:+/–]; $n = 5$) embryos. Compared with the LSK cells recovered from Tg:+/+ and Tg:+/– FLs (2.2×10^4 to 5.7×10^4 and 1.3×10^4 to 4×10^4, respectively), very few LSK cells (98–477) were recovered from Tg^{VE}:*Gata2*$^{-/fl}$ (Tg:–/fl; $n = 4$) embryos. Compared with the LSKS cells recovered from Tg:+/+ and Tg:+/– FLs (1.2×10^3 to 4×10^3 and 0.5×10^2 to 1.6×10^2, respectively), a minuscule number of LSKS cells were recovered from Tg^{VE}:*Gata2*$^{-/fl}$ FLs. Although there appears to be little difference in mCh^{+} LSK and LSKS percentages in Tx-treated Tg^{VE}:+/+ and Tg^{VE}:+/– FLs, the absolute number indeed drops by half.

(M3434, Stem Cell Technologies). *Gata2* heterozygotes (*Gata2*$^{+/-}$, Tg^{VE}:*Gata2*$^{+/fl}$, $n = 13$) and Tg^{VE}:*Gata2*$^{-/fl}$ embryos ($n = 6$) also generated lower numbers of erythroid, myeloid, and mixed-lineage colonies (Figure 3B). Notably, Tx-treated Tg^{VE}:*Gata2*$^{-/fl}$ FL cells failed to generate BFU-E, CFU-G/M/GM, or CFU-GEMM colonies (Figure 3B), initially suggesting that a very early definitive hematopoietic progenitor compartment was severely compromised in Tx-treated Tg^{VE}:*Gata2*$^{-/fl}$ embryos.

Successful Cre-mediated excision of the *Gata2* floxed allele was determined at the RNA and genomic DNA levels. Remaining GATA-2 transcript abundance (if any) in Tx-treated FL samples that were used for CFU assays was examined by RT-qPCR. In Tg^{VE}:*Gata2*$^{-/fl}$ FL cells, *Gata2* mRNA (relative to endogenous *Hprt* mRNA) was reduced to 15% of that in wild-type embryos (Figure 3C). We also quantified Cre-mediated excision of the floxed *Gata2* allele using qPCR assay to detect the presence of exon 5 (the one flanked by *loxP* sites in the floxed *Gata2* allele, normalized to *Actin*) in genomic DNAs extracted from individual colonies isolated from Tx-treated Tg^{VE}:*Gata2*$^{+/fl}$ methylcellulose cultures. Of the 35 Tg^{VE}:*Gata2*$^{+/fl}$ individual colonies analyzed, *Gata2* exon 5 was detected at 58% ± 6% relative to the wild-type control. Hence, the calculated excision efficiency of the single floxed *Gata2* allele achieved was 84% (Figure 3D and Supplemental Figure 2). Together, our results confirmed that the in vivo induction of CreERT^2 activity led to effective *Gata2* inactivation in Tg^{VE}:*Gata2*$^{-/fl}$ embryos.

Since the in vitro colony-forming assays could not be used to pinpoint where the defect was in the affected progenitor population (i.e., in multipotent hematopoietic progenitors or even more primitive HSCs), more precise and quantitative hematopoietic lineage analysis was undertaken using flow cytometry. To inves-

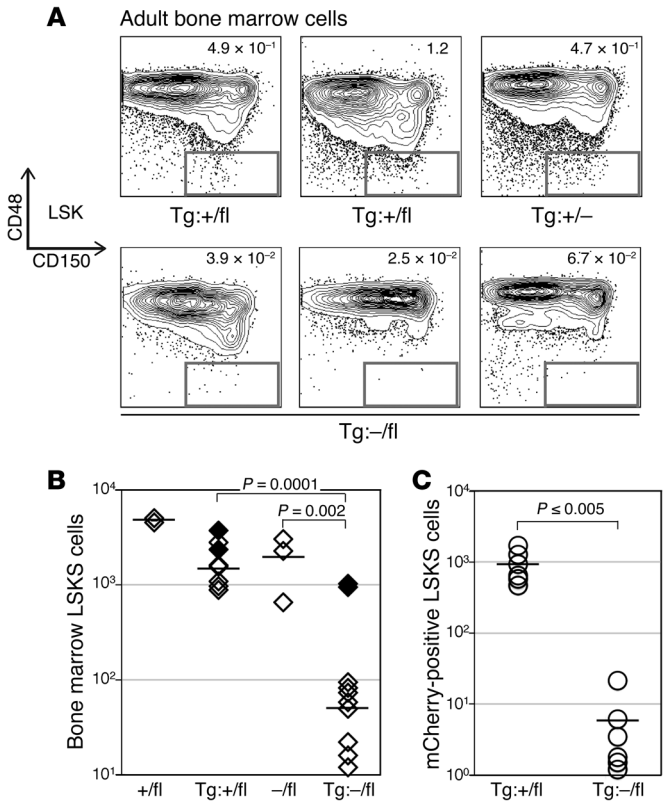

Figure 5
Severely attenuated HSC recovery from Tx-treated Tg^{VE}:*Gata2*$^{-/fl}$ adult BM. (**A**) Adult mice (8–12 weeks of age) were gavaged with Tx (5 mg/d) or sunflower oil for 5 consecutive days. BM cells were isolated 48 hours after the final Tx administration and then stained with various antibodies directed against cell surface antigens prior to analyses. Representative contour plots for the LSKS (LSK Slam; LSKCD150$^+$CD48$^-$) fractions in Tx-treated control (2 Tg^{VE}:*Gata2*$^{+/fl}$ and 1 Tg^{VE}:*Gata2*$^{+/-}$) mice and in 3 Tx-treated Tg^{VE}:*Gata2*$^{-/fl}$ compound heterozygous adult mice are shown. The percentage of LSKS cells in each gated area (boxed) is shown. (**B**) Distribution of highly purified HSCs isolated from Tx-treated (white) or mock-treated (black) control or test mice (2 tibias plus 2 femurs). *Gata2*$^{+/fl}$ and *Gata2*$^{-/fl}$ adult mice without or with Tg^{VE} were gavaged with Tx (5 mg/d) or sunflower oil for 5 consecutive days. The 4 groups of mice are designated as follows: *Gata2*$^{+/fl}$, +/fl (n = 2); Tg^{VE}:*Gata2*$^{+/fl}$, Tg:+/fl (n = 8); *Gata2*$^{-/fl}$, –/fl (n = 3); and Tg^{VE}:*Gata2*$^{-/fl}$, Tg:–/fl (n = 10). Data were compiled from 3 independent experiments. The ordinate axis is on a log scale; the horizontal bars represent the mean number of LSKS cells in Tx-treated mice of each genotype. Statistical significance was determined by Student's t test. (**C**) Absolute number of adult BM LSKS cells in each mouse (2 tibias plus 2 femurs) expressing mCh (ordinate axis is log scale). The number of mCh-expressing cells in the Tg^{VE}:*Gata2*$^{+/fl}$ versus Tg^{VE}:*Gata2*$^{-/fl}$ fractions differs by 2–3 orders of magnitude. The horizontal bars represent the mean number of mCh-positive LSKS cells in Tx-treated mice of each genotype. Statistical significance was determined by Student's t test.

tigate in greater depth the hypothesis that the VE enhancer regulates Cre-mediated inactivation of *Gata2*, thereby ablating a very early hematopoietic progenitor compartment, we isolated E14.5 FLs from embryos that had been administered Tx daily from E9 through E11 and then performed flow cytometry to determine the immunophenotype corresponding to different early progenitor populations. The combinatorial analysis of a subset of Slam family receptors (CD150 and CD48) in conjunction with conventional HSC surface markers (mature hematopoietic lineage–negative, Sca-1–positive, and c-Kit–positive [LSK]) facilitates the identification of a highly enriched HSC cellular fraction in which 1 in every 2.1 recovered cells is capable of conferring long-term multilineage reconstitution in lethally irradiated host animals (32, 33).

We found that Tx-treated embryos bearing a single *Gata2* null allele (Tg^{VE}:*Gata2*$^{+/-}$, Tg^{VE}:*Gata2*$^{+/fl}$, *Gata2*$^{-/fl}$; n = 9) had reduced LSK and LSKS (lin$^-$Sca-1$^+$c-Kit$^+$CD150$^+$CD48$^-$) cells when compared with wild-type or pseudo-wild-type (*Gata2*$^{+/+}$, Tg^{VE}:*Gata2*$^{+/+}$, *Gata2*$^{+/fl}$; n = 6) embryos (Figure 4). The total number of HSCs recovered from Tx-treated embryos bearing two wild-type alleles was between 2.2×10^4 to 5.7×10^4 (LSK) and 1.2×10^3 to 4.6×10^3 (LSKS), whereas only 1.3×10^4 to 4.0×10^4 (LSK) or 0.5×10^3 to 1.6×10^3 (LSKS) cells were recovered from Tx-treated embryos bearing a single *Gata2* null allele. These data mirrored previous reports showing that *Gata2* haploinsufficiency results in compromised HSC homeostasis (13, 14). Intriguingly, we found that when Tg^{VE}:*Gata2*$^{-/fl}$ embryos (n = 4) were administered Tx between E9 and E11, both the LSK and the more highly HSC-enriched LSKS populations displayed an exponential decline (Figure 4, C–E). A small number of LSK cells (i.e., 98–477) were recovered from Tx-treated Tg^{VE}:*Gata2*$^{-/fl}$ (Figure 4C; n = 4) embryos, and likewise a minuscule number of LSKS cells were recovered from these FLs (Figure 4D). We obtained the same results when Tx was administered later during gestation (between E11 and E13), at a time during embryogenesis when definitive hematopoiesis was already fully engaged (Figure 4B). This is consistent with the observation that in embryos hemizygous for an active Tg^{VE} transgene, a majority of both LSK and LSKS cells were mCh$^+$ (64% ± 4% and 87% ± 6%, respectively, n = 7; Figure 4E and data not shown). We conclude that the loss of GATA-2 activity in those tissues regulated by the *Gata2* VE enhancer results in a virtually complete loss of HSCs in the most highly refined fraction of fetal HSCs, revealing for the first time to our knowledge the localization of a transcriptional regulatory element that is capable of controlling HSC activity of the *Gata2* gene.

VE-regulated Gata2 loss in Tx-treated mice depletes BM HSCs. To determine whether the *Gata2* VE enhancer displays stage-specific differential activity among definitive HSCs, we asked whether the Tg^{VE} transgene would ablate *Gata2* expression in adult BM HSCs as it did in FL HSCs, distinct but closely related definitive HSC populations (34). *Gata2*$^{-/fl}$ and *Gata2*$^{+/fl}$ adult mice (without or with the Tg^{VE}, from 8 to 12 weeks of age) were gavaged with Tx (5 mg/d) for 5 consecutive days. Two days after the final Tx administration, BM cells were harvested and analyzed by flow cytometry. Once again, we employed the immunophenotype defined by Kiel et al. (32) to define the most enriched definitive HSC population (LSKS cells).

In comparing the absolute LSK and LSKS cell numbers between Tg^{VE}:*Gata2*$^{+/fl}$ and Tg^{VE}:*Gata2*$^{-/fl}$ adult mice that had not been administered Tx (Figure 5B and data not shown) and between *Gata2*$^{+/fl}$ and *Gata2*$^{-/fl}$ mice exposed to Tx (Figure 5B and data not shown), we again noted that reduced *Gata2* gene dosage correlated

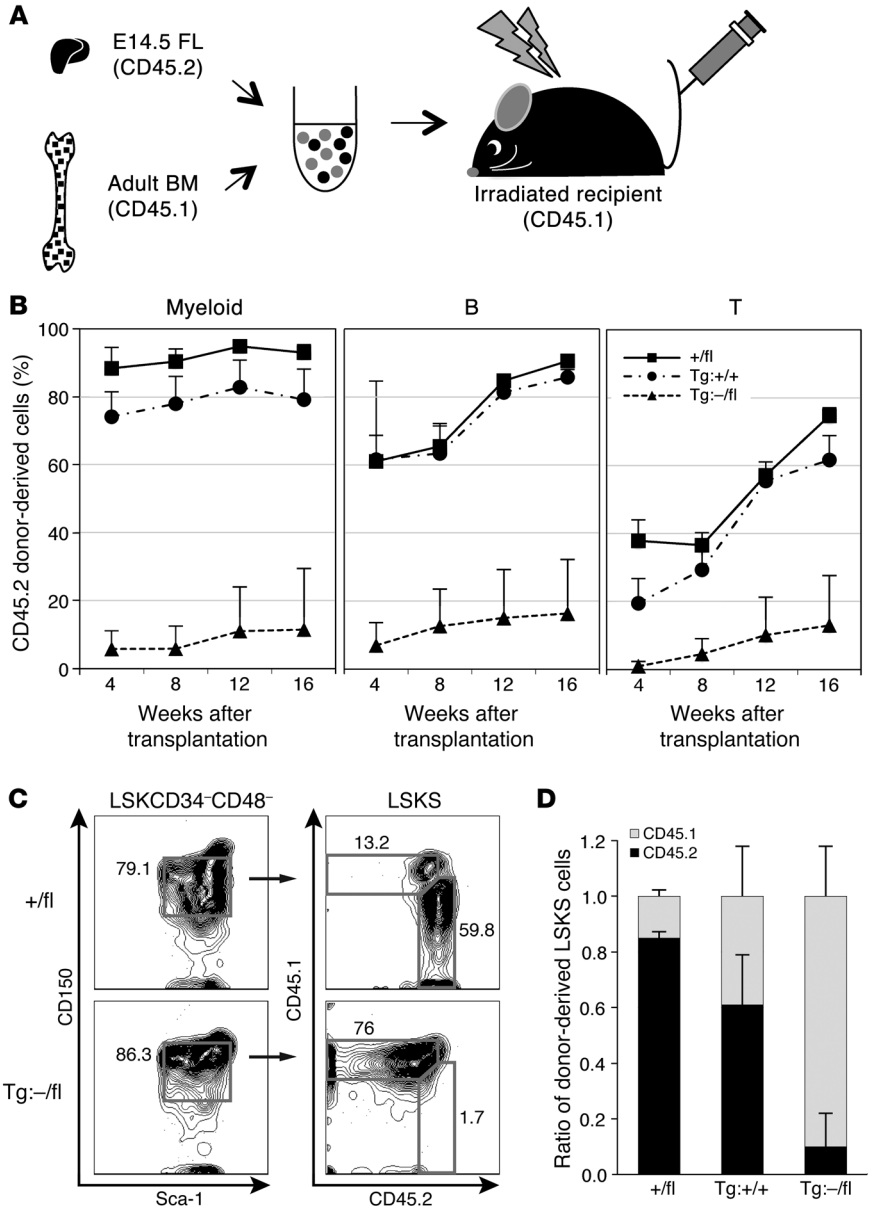

Figure 6

Long-term hematopoietic reconstitution of Tx-treated E14.5 Tg^{VE}:*Gata2*$^{-/fl}$ FL cells is severely compromised. (**A**) Strategy for competitive reconstitution of lethally irradiated CD45.1 adult mice. 5 × 10^5 E14.5 total FL cells from control (*Gata2*$^{+/fl}$ [*n* = 1], Tg^{VE}:*Gata2*$^{+/+}$ [*n* = 3], or Tg^{VE}:*Gata2*$^{-/fl}$ [*n* = 2]) Tx-treated CD45.2 embryos were transplanted together with 5 × 10^5 CD45.1 adult BM cells. FL cells from each embryo were transplanted into 5 recipients. (**B**) Donor chimerism in the peripheral blood was assessed by flow cytometry using anti-CD45.1–PECy7 and anti-CD45.2–APC antibodies from 4 to 16 weeks after transplantation. CD45.2 donor cell contribution (mean ± SD) from 2 independent experiments is shown. Unlike the robust peripheral blood reconstitution by control FL cells in transplant recipients, Tg^{VE}:*Gata2*$^{-/fl}$ FL cells barely reconstituted their irradiated hosts. Transplant recipients: *Gata2*$^{+/fl}$ (*n* = 5), Tg^{VE}:*Gata2*$^{+/+}$ (*n* = 15), Tg^{VE}:*Gata2*$^{-/fl}$ (*n* = 10). (**C** and **D**) Sixteen weeks after transplantation, BM cells were harvested from each mouse (2 tibias plus 2 femurs), and the ratios of CD45.1 to CD45.2 LSKS cells were determined by flow cytometry. Representative contour plots of irradiated CD45.1 recipients that received *Gata2*$^{+/fl}$ (+/fl) or Tg:*Gata2*$^{-/fl}$ (Tg:–/fl) FL cells are shown (**C**). Note the conspicuous absence of CD45.2 FL donor-derived LSKS cells in the latter representative recipient. The average ratio of CD45.1 to CD45.2 LSKS cells in transplant recipients that received *Gata2*$^{+/fl}$ (+/fl; *n* = 5), Tg:*Gata2*$^{+/+}$ (Tg:+/+; *n* = 5), or Tg:*Gata2*$^{-/fl}$ (Tg:–/fl; *n* = 10) is shown (**D**). Note that in the latter group of recipients, the majority of LSKS cells are not derived from FL. Data represent mean ± SD.

perfectly with diminished LSKS cell number. This is reminiscent of the same phenomenon observed in E14.5 FL HSCs (Figure 4) that was also previously reported by others (14). When *Gata2*$^{+/fl}$ and *Gata2*$^{-/fl}$ mice bearing the Tg^{VE} were exposed to Tx, we saw a further precipitous decline in the LSKS population as a consequence of reduced GATA-2 activity (Figure 5, A–C). Explicitly, in Tx-treated adult Tg^{VE}:*Gata2*$^{-/fl}$ mice, the LSKS population was depleted by approximately 2 orders of magnitude within a week after the first Tx exposure (Figure 5, B and C). Thus, the *Gata2* VE enhancer is functional in both FL and adult BM definitive HSCs, and loss of GATA-2 adversely impacts HSC survival and/or proliferation.

Defective long-term hematopoietic reconstitution from Tg^{VE}:Gata2$^{-/fl}$ FL cells. To functionally detect HSCs in Tx-treated mice, we performed competitive repopulation assays. Total CD45.2 FL cells (5 × 10^5) from control (*Gata2*$^{+/fl}$ [*n* = 1] or Tg^{VE}:*Gata2*$^{+/+}$ [*n* = 3]) or from Tg^{VE}:*Gata2*$^{-/fl}$ (*n* = 2) E14.5 embryos, all of which had been exposed to Tx from E9 to E11, were coinjected at a 1:1 ratio with wild-type CD45.1 adult BM cells (5 × 10^5) into lethally irradiated CD45.1 animals (5 mice per group; Figure 6A). Peripheral blood reconstitution from CD45.2 donor FL-derived cells was monitored from week 4 to 16 after transplantation. In all animals receiving *Gata2*$^{+/fl}$ (*n* = 5) or Tg^{VE}:*Gata2*$^{+/+}$ (*n* = 15) FL cell transplants, the FL-derived donor cells contributed to the myeloid (>80%), B (>80%), and T (>60%) lymphoid lineages in the peripheral blood (Figure 6B and Supplemental Figure 3A). In contrast, in transplant recipients injected with Tx-treated Tg^{VE}:*Gata2*$^{-/fl}$ FL cells, only a weak multilineage reconstitution was observed in most animals (8 of 10), while some level (<30%) of multilineage reconstitution was seen in the remaining two animals (Figure 6B, Supplemental Figure 3A, and data not shown).

When we analyzed the highly HSC-enriched LSKS fraction in the BM of transplant recipients, we found that in control animals, CD45.2 FL–derived LSKS constituted the major population (60%–80%; Figure 6, C and D). In contrast, 8 of 10 animals that

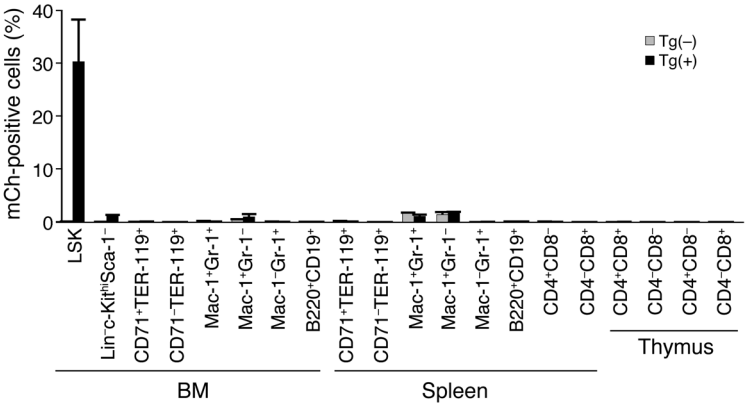

Figure 7

mCh expression is restricted predominantly to the LSK fraction in adult BM. Cells were isolated from BM, spleen, and thymus of wild-type adult mice without Tg^{VE} ($n = 2$; gray bars) or hemizygous for Tg^{VE} ($n = 4$; black bars) and then stained with various antibodies directed against developmental cell surface antigens prior to flow cytometric analyses. The percentages of mCh-positive cells within the immature (LSK and lin⁻Sca-1⁻c-Kit^{hi}) and committed erythroid, myeloid, B lymphoid, or T lymphoid cell compartments are summarized. The latter 4 committed lineages were characterized using pairs of antibodies (CD71 and TER-119, Mac1 and Gr-1, B220 and CD19, CD4 and CD8), respectively. Most conspicuously, mCh is expressed at 30- to 1,000-fold lower abundance in all mature hematopoietic lineages, but is robustly expressed exclusively in adult BM LSK cells.

received Tg^{VE}:*Gata2*$^{-/fl}$ FL cells had more than 90% of the LSKS fraction derived from wild-type CD45.1 BM cells. The two remaining transplant animals, in which some CD45.2 progenitor cells were detected in the peripheral blood (Figure 6B and Supplemental Figure 3A), had some (20% and 40%) CD45.2 FL-derived LSKS in their BM (Figure 6, C and D, Supplemental Figure 3B). When we analyzed FACS-sorted CD45.2-positive LSK cells from the latter two animals by qPCR, we found that these cells indeed contained an intact *Gata2*^{fl} allele (data not shown), indicating that approximately 20% of LSKS cells per Tg^{VE}:*Gata2*$^{-/fl}$ embryo had escaped VECre-mediated *Gata2* inactivation, in good agreement with the efficiency of conditional GATA-2 loss (Figure 3).

Within the adult hematopoietic cell hierarchy, we noted that mCh epifluorescence was absent in mature lymphoid, myeloid, and erythroid lineages isolated from the BM, spleen, or thymi of wild-type adult mice harboring Tg^{VE} (Figure 7), in stark contrast to endogenous GATA-2 expression in the erythroid and myeloid compartments (35, 36). Most conspicuously, mCh expression was almost entirely restricted to the BM LSK fraction that contained all stem cells. These additional data further underscored the highly restricted and early-acting (within hematopoietic lineages) activity of the *Gata2* VE enhancer within the hematopoietic cell hierarchy. Thus, these data demonstrate that induction of VE-regulated Cre leads to functional depletion of HSCs and that the *Gata2* VE element possesses HSC- and early progenitor–restricted enhancer activity.

Physiological consequences of Gata2 conditional loss of function during embryogenesis. We noted that live Tg^{VE}:*Gata2*$^{-/fl}$ embryos began to appear edematous by E13.5, and they invariably developed severe subcutaneous edema, hemorrhage, and anemia and died by E16.5 (Figure 8A, arrows). The identical phenotype was encountered when we employed a second, independent conditional Cre transgenic line (Tg^{VE56}; Figure 1B and legend to Figure 8). Importantly, we did not observe these phenotypes in Tx-treated embryos that did not bear a Cre transgene, and therefore we were confident that the phenotypes were not due to Tx toxicity; the acquisition of these phenotypes correlated only with Cre induction in the embryos that co-inherited *Gata2* null and floxed alleles. Further experiments performed with only a single Tx delivery on day 9 after fertilization or after 3 consecutive daily doses from E11 to E13, instead of the generally employed Tx regimen of 3 consecutive daily doses from E9 to E11, generated the identical phenotypes of anemia, edema, and hemorrhaging in Tg^{VE}:*Gata2*$^{-/fl}$ embryos. PCR genotyping of yolk sac genomic DNAs confirmed the conversion of the *Gata2* floxed allele to the *Gata2* exon 5–deleted allele (*Gata2*$^{\Delta}$, Figure 8B). The *Gata2*$^{\Delta}$ amplicon was detected exclusively in embryos bearing both the *Gata2* floxed allele and Tg^{VE} from dams that had been treated with Tx. Since CreERT^2 expression is restricted to endothelial cells in the yolk sac, the (unaltered) *Gata2* floxed allele was still detected in total yolk sac genomic DNA of Tx-treated Tg^{VE}:*Gata2*$^{-/fl}$ embryos (Figure 8B). Thus, the final phenotype revealed by employing this binary conditional inactivation strategy was that loss of GATA-2 in the endothelial lineage leads to massive mid-gestational hemorrhage, edema, and anemia, followed shortly thereafter by embryonic demise by around E16.5.

We noted massive blood pooling in the vicinity of the jugular lymph sacs in E14.5 Tx-treated mutant, but not control, embryos (Figure 9, A and B). Detailed examination of serial histological sections of E13.5 Tx-treated (from E9 to E11) embryos revealed that in the control embryo, the jugular lymph sac was distinctly separated from the jugular vein, while in the mutant only a single vessel lumen could be found (Figure 9, C–E and I). When we examined serial sections of Tg^{VE}:*Gata2*$^{-/fl}$ embryos more anteriorly and posteriorly, we saw that the lymph sacs appeared hypoplastic compared with that of the control embryo (Figure 9, E and F). Additionally, erythrocytes were aberrantly present in the lymph sacs (Figure 9, G and H) of the E13.5 Tg^{VE}:*Gata2*$^{-/fl}$ mutant embryo, which typically had not presented visibly outward signs of gross hemorrhage by this gestational day (Figure 8). Thus, employing this binary conditional inactivation strategy revealed yet another striking phenotype: GATA-2 function is required for proper lymphatic morphogenesis during embryonic development.

Discussion

The study of *Gata2* transcriptional regulation in hematopoiesis has a long and storied history. More than a decade ago, we discovered that a 271-kbp *Gata2* yeast artificial chromosome (YAC) transgene, which circumscribed genomic sequences from –198 kbp to +73 kbp (with respect to the translational start site) of the *Gata2* locus, could fully rescue the embryonic lethality in *Gata2*$^{-/-}$ embryos (3). Hence, this YAC functionally defined the genomic limits of the *Gata2* locus that contained all of the regulatory element(s) required for fully elaborating primitive and definitive hematopoiesis, but the YAC only incompletely rescued all of the GATA-2 functions, since the P0 pups died from incomplete patterning of the urogenital system (3, 9, 20).

In contemporaneous studies, Kobayashi-Osaki et al. (37) reported that the *Gata2* GATA-2–EHRD element, located 3.1 kbp 5′ to the *Gata2* 1S first exon, was capable of directing GFP reporter gene

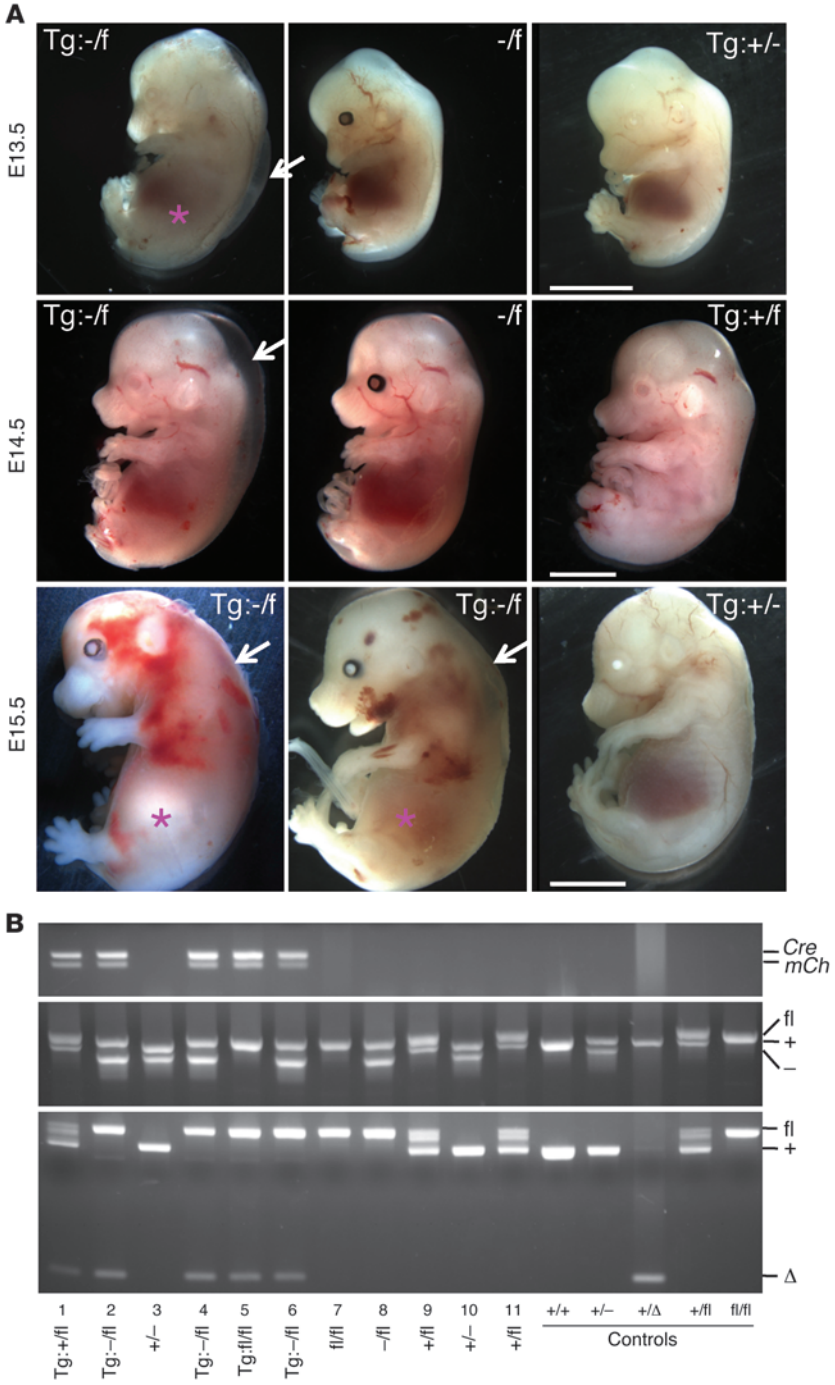

Figure 8

Tx-treated Tg^{VE}:*Gata2*$^{–/fl}$ embryos exhibit anemia, edema, hemorrhage, and late-embryonic lethality. (**A**) *Gata2*$^{+/fl}$ female mice were intercrossed with Tg^{VE}:*Gata2*$^{+/–}$ compound transgenic males. Embryos were collected from pregnant dams that were gavaged with Tx between E9 and E11. Anemia, edema, and hemorrhage were detected in Tx-treated Tg^{VE}:*Gata2*$^{–/fl}$ (Tg:–/f) embryos, but not in any other genotype control littermates, of which some are shown here (*Gata2*$^{–/fl}$, Tg^{VE}:*Gata2*$^{+/–}$, Tg^{VE}:*Gata2*$^{+/fl}$ [–/f, Tg:+/–, Tg:+/f, respectively]), beginning around E13.5 and progressively increasing in severity before they succumbed to lethality and necrosis by E15.5–E16.5. Arrows: subcutaneous edema in Tg^{VE}:*Gata2*$^{–/fl}$ embryos. Note the visibly paler FLs (magenta asterisks) in Tx-treated E13.5 and E15.5 Tg^{VE}:*Gata2*$^{–/fl}$ embryos in comparison to Tx-treated controls. (A patch of hemorrhage in the E14.5 Tg^{VE}:*Gata2*$^{–/fl}$ embryo visually obscured its pallid liver). These phenotypes were reproducible using either of two transgenic lines (Tg^{VE56}: E14.5 embryos; Tg^{VE62}: E13.5 and E15.5 embryos). Further experiments performed with only a single Tx delivery on E9 (data not shown) or after 3 consecutive doses from E11 to E13 instead of E9 to E11 generated the same phenotypes (anemia, edema, hemorrhaging) in Tg^{VE}:*Gata2*$^{–/fl}$ embryos. Scale bar: 0.5 mm. (**B**) Genotyping of a (large) representative E13.5 litter collected from a Tx-gavaged *Gata2*$^{–/fl}$ female intercrossed with a Tg^{VE}:*Gata2*$^{+/fl}$ adult male. Yolk sac genomic DNAs were used in separate PCR reactions to specifically detect the Cre and mCh transgenes (top), 3 *Gata2* alleles (fl, wild-type [+], or knockout [–]; middle) and the Cre-mediated *Gata2* exon 5–deleted allele (Δ; bottom). The *Gata2*^{Δ} amplicon was only detected in embryos bearing both the *Gata2*^{fl} allele and Tg^{VE}. Since CreERT^2 expression is restricted to endothelial cells in the yolk sac, the PCR amplicon derived from the unrecombined *Gata2*^{fl} allele was detected in total yolk sac genomic DNA of Tx-treated Tg^{VE}:*Gata2*$^{–/fl}$ embryos. To generate the *Gata2*^{Δ} allele as a positive control, the *Gata2*$^{+/fl}$ mouse was interbred with the ubiquitously expressed AyuI-Cre transgenic mouse (21). Sequences of primers used for PCR genotyping are listed in Supplemental Table 1.

expression within the para-aortic splanchnopleura, the immediate developmental precursor of the aorta-gonad-mesonephros (AGM), from which definitive HSCs first emerge in mice (38). This promoter-proximal element was later shown to modulate GATA-2 abundance in E12.5 FL HSCs and its immature progenitor populations, but not in adult HSCs (39).

Suspicions regarding the potential complexity of *Gata2* hematopoietic transcriptional regulation were underscored when Bresnick and colleagues identified 5 GATA motif–bearing regions (–77, –3.9, –2.8, –1.8, and +9.5 relative to the *Gata2* 1S transcription start site) that are bound by GATA-2 but are replaced by GATA-1 during erythroid differentiation (40), suggesting that each of these "GATA switch" sites might also play roles in regulating *Gata2* expression during hematopoiesis. When either the –1.8 or –2.8 site was systemically deleted from the germ line, GATA-2 transcripts were altered in HSCs, but this did not translate into a detectable change in HSC number (39, 41); this implies that other regulatory element(s) within the *Gata2* locus are responsible for its HSC activity.

In our continuing efforts to elucidate the transcriptional regulation of GATA-2, we have in the past examined reporter gene expression using large (yeast and bacterial artificial chromosomes) and small (plasmid) expression vectors in transgenic studies. As a

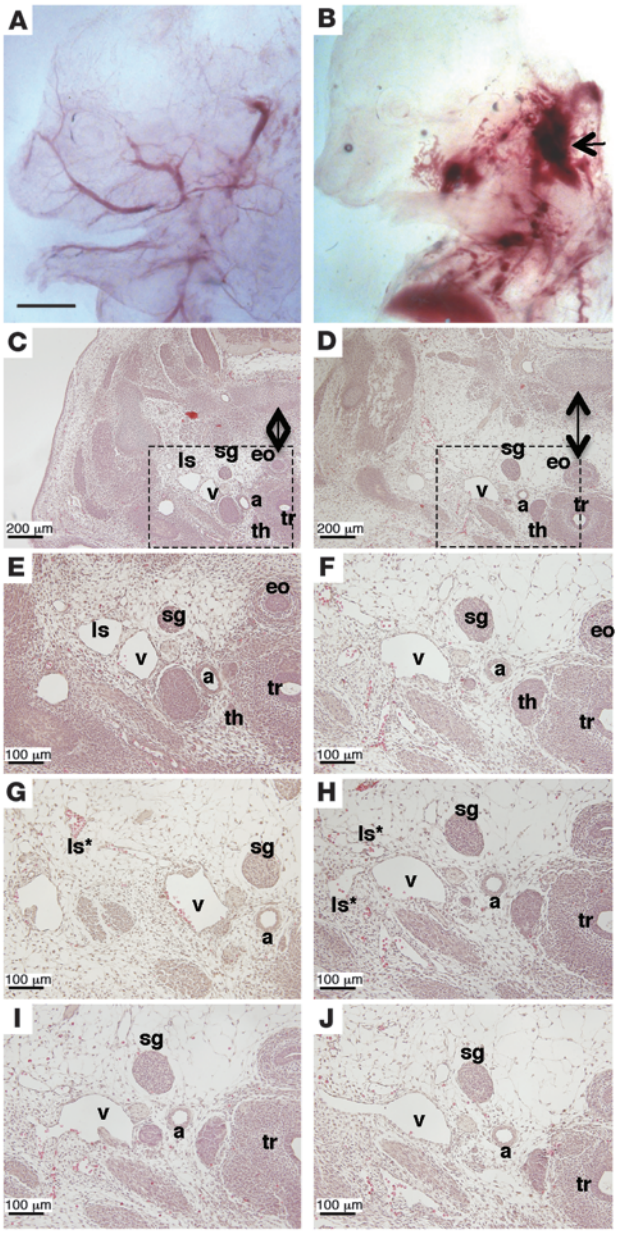

Figure 9

Aberrant lymphatic development in Tg^{VE}:*Gata2*$^{-/fl}$ embryos. (**A** and **B**) Tx-treated E14.5 *Gata2*$^{+/fl}$ (**A**) and Tg^{VE}:*Gata2*$^{-/fl}$ (**B**) embryos were fixed in 4% paraformaldehyde and then gradually cleared in benzyl benzoate:benzyl alcohol for whole-mount photography. Note the blood-engorged jugulo-axillary lymph sac (arrow) in the Tg^{VE}:*Gata2*$^{-/fl}$, but in not in the control, embryo. (**C**–**F**) Transverse paraffin sections (6 μM) of an E13.5 Tx-treated (E9–E11) Tg^{VE}:*Gata2*$^{+/+}$ (**C** and **E**) or Tg^{VE}:*Gata2*$^{-/fl}$ (**D** and **F**–**J**) embryos were stained with H&E. While in the control embryo, the jugular vein (v) is distinctly separated from the jugular lymph sac (ls) at the axial level of the thyroid gland (th, **C**; an enlarged view of boxed area is shown in **E**), only a single vessel lumen is observed in the Tx-treated Tg^{VE}:*Gata2*$^{-/fl}$ embryo (**D**; enlarged view of boxed area is shown in **F**). **C** and **D** were taken at the same magnification; the tissue edema in Tg^{VE}:*Gata2*$^{-/fl}$ embryo did not permit coverage of the entire area in the microscopic field. By following serial sections anteriorly (**G** and **H**) and posteriorly (**I** and **J**) of the section shown in **F**, it appeared that the jugular vein remained abnormally connected to the lymphatic system. Note the interstitial edema (indicated by the arrow; **B**) and the aberrant presence of erythrocytes in the lymph sacs (indicated by asterisks) before the onset of visible hemorrhage (e.g., see Figure 8) of E13.5 Tx-treated Tg^{VE}:*Gata2*$^{-/fl}$ embryo. a, carotid artery; eo, esophagus; sg, sympathetic ganglion; tr, trachea; va, vagal nerve trunk. Scale bars: 1 mm (**A** and **B**), 200 μm (**C** and **D**), 100 μm (**E**–**J**).

result of these analyses, we previously identified and characterized an intronic *Gata2* VE enhancer predominantly as an endothelial regulatory element using lacZ-tagged plasmid expression vectors in founder transgenic studies (5). The data presented here demonstrate that the *Gata2* VE enhancer is transcriptionally active in both FL and adult BM HSCs and that VE-regulated conditional *Gata2* loss leads to massive depletion of the most highly purified immunophenotypic fetal and adult definitive HSCs. On closer scrutiny, we noted that VE-regulated mCh expression co-segregated with most (87% ± 6%) of the most highly purified fraction of Tg^{VE}-bearing wild-type E14.5 FL LSKS HSCs (Figure 4E), while only about 60% of the Tg^{VE}-bearing wild-type LSKS population recovered from adult BM expressed mCh (Figure 5C). This difference in mCh expression in the most highly purified fraction of FL versus adult BM HSCs could reflect the differential activity of the *Gata2* VE enhancer in the HSC cellular milieu at different developmental stages; alternatively, the data could as easily be interpreted to support the hypothesis that the adult BM HSC compartment is intrinsically more heterogeneous than the fetal compartment, a contention strongly supported by recent literature (42–44). The data could also be explained simply as a consequence of diminished levels of mCh expression in adult LSKS HSC or altered stability of the protein in (perhaps longer-lived) adult LSKS cells.

The constitutive loss of GATA-2 that leads to early embryonic lethality by E10.5 has been attributed to primitive hematopoietic failure (2, 3). Further insight into a role for GATA-2 in definitive hematopoiesis was gleaned from the examination of null mutant embryonic stem cells and their contribution to in vitro differentiation or to definitive hematopoiesis in reconstituted chimeras, where it was deductively concluded that GATA-2 is required for the proliferation and/or survival of HSCs (12). More recent analyses of *Gata2* heterozygous mutant mice clearly demonstrated a quantitative reduction in HSC number and compromised HSC function in competitive BM reconstitution experiments (13, 14). Here, using a combinatorial conditional loss-of-function strategy, we were able to directly and formally demonstrate that GATA-2 is vital for immunophenotypic as well as functional HSC recovery from both mid-gestational embryos and adults. In light of the negligible effects of the –1.8 and –2.8 kb promoter *Gata2* mutations on HSCs (above), it will be interesting to determine the consequence of deleting the *Gata2* VE enhancer singly or in combination with other putative *Gata2* regulatory elements to ascertain their individual and combinatorial contribution to *Gata2* transcription in HSCs and, in particular, whether the VE HSC activity described here is a unique or redundant function within the locus.

In our previous and in current studies, we noted the presence of X-gal–stained hematopoietic cells that appeared to be budding into the lumen of the dorsal aorta in E10.5 embryos, possibly hinting that this enhancer might be active in hemogenic endothelium or hemangioblasts, the presumptive progenitor cell common to the endothelial and hematopoietic lineages. Indeed, using blast colony–forming cells derived from embryonic stem

cells, Lugus et al. showed that temporally sensitive, conditionally forced induction of GATA-2 led to a transient expansion of hemangioblasts in cell culture (45). Whether it is required for the development of an even earlier-stage, common progenitor cell (30, 45) will require additional study.

While GATA-2 appears not to be required for endothelial patterning into the initial primary vasculature (as evident in E10.5 *Gata2* homozygous null embryos), it may be necessary for the elaboration of the mature vasculature later during embryogenesis. At the time of embryonic demise at E16.5, the binary conditionally inactivated *Gata2* mutant mice displayed severe subcutaneous edema and extensive hemorrhage. We show that the VE is active in the cardinal vein, where endothelial precursor cells with potential to differentiate into LECs are generated (26), and in nascent LECs that have sprouted from the cardinal vein (5). Robust GATA-2 expression has also been reported in E16.5 and adult murine lymphatic vessel and lymphatic valves (17). The abnormal accumulation of blood in the jugular lymph sacs in Tx-treated Tg^{VE}:$Gata2^{-/fl}$ embryos prompted us to histologically examine their embryonic lymphatic vasculature. Curiously, we found that in Tx-treated E13.5 Tg^{VE}:$Gata2^{-/fl}$ embryos, the lymphatic and blood vascular systems remained aberrantly connected, unlike in control embryos. Interestingly, there have been several recent reports of primary lymphedema in patients with either Emberger or monocytopenia and mycobacterial infection (MonoMAC) syndrome due to *GATA2* mutations (16–18).

Much progress has been made over the last decade with regard to understanding embryonic lymphatic vascular development, and numerous genes that impact this morphogenic process have now been identified (46). In particular, the blood-lymphatic mixing phenotype had been reported in mice with mutations that affect podoplanin (47), *Ruxn1* (26), *Meis1* (48), *Syk* (49), *Slp76* (50), and *Plcg2* (51). A number of these mutants have platelet deficiency or dysfunction, as there is accumulating evidence that platelets play a central role in lympho-venous partitioning (46). Whether this pathophysiological developmental aberration in Tx-treated Tg^{VE}:$Gata2^{-/fl}$ embryos is due to loss of GATA-2 expression in the hematopoietic and/or lymphatic endothelial lineage will require further investigation. It will be of interest to now investigate the role and mechanism(s) by which GATA-2 intersects with the developmental programs specifying lymphangiogenic differentiation.

Methods

Expression plasmid construction. The lacZ insert in pTKSXβ (5), containing a 1.2-kbp SfiI/XbaI *Gata2* intron 4 enhancer fragment in pTKβ vector (Clontech), was removed by NotI digestion and replaced with a Klenow-treated EcoR1 $CreER^{T2}$ fragment (52) or a Klenow-treated BamHI/NotI fragment encoding the fluorescent reporter gene mCh (Clontech). Both resultant plasmids were sequentially treated with PvuII/SphI and Klenow polymerase. The excised inserts were separately ligated into PacI-digested pIV vector, which contained duplicated 1.2-kbp chicken HS4 insulators (53) sequentially cloned into the polylinker (SmaI and PmeI) sites of pNEB193 (NEB). The VECre and VEmCherry expression plasmids were verified by sequencing during and at the completion of construction.

Mutant mice. Trangenic mice were generated by the the Transgenic Animal Model Core at the University of Michigan Medical School. Plasmids VECre and VEmCherry were digested with FspI, purified, and microinjected (1:1 ratio) into (C57BL/6 × SJL) F_1 fertilized eggs. Transgenic animals were identified by PCR detection of Cre and mCh (Supplemental Table 1) using genomic DNAs isolated from tail snips as template.

For mouse lines that stably transmitted both Cre and mCh transgenes (referred to as Tg^{VE} lines), F_2–F_5 progeny were examined for Cre transgene copy number, Cre mRNA levels, and mCh fluorescence. For Cre transgene copy number analysis, tail snip genomic DNAs were used as template in SYBR Green qPCR as described previously (20) using endogenous *Actin* as a normalization control. Genomic DNAs from mice that were wild-type, heterozygous, or homozygous for the AyuI-Cre knock-in allele (21) were included as copy number controls for the Cre qPCR assays (data not shown). For determining Cre transcript levels, total RNAs were isolated from vascularized tissues (heart and kidney) of neonatal pups that were Cre transgene positive. Reverse transcription and SYBR Green qPCR were performed as previously detailed (54), and Cre mRNA abundance was expressed relative to endothelia-specific *Flk1* mRNA. All primer pairs used for qPCR are listed in Supplemental Table 1.

Selected Tg^{VE} lines (62 and 56) that coexpressed intense endothelia-specific mCh fluorescence and robust Cre mRNAs were independently mated with *R26R* (25), $Tg^{Tie2.GFP}$ transgenic (24), or $Gata2^{+/gfp}$ (21) mice (in which a *gfp* gene was inserted at the *Gata2* translational start site) to generate E10.5–E12.5 compound transgenic embryos. Embryos from the first intercross were isolated from Tx-gavaged pregnant females and processed for X-gal staining and then subjected to whole-mount photography or cryosectioning and counterstaining with nuclear fast red (5). E10.5 Tg^{VE}:$Tg^{Tie2.gfp}$ and Tg^{VE}:$Gata2^{+/gfp}$ embryos were examined by fluorescence confocal microscopy. Genomic DNAs from yolk sacs or embryonic tails were used for PCR genotyping (21, 24, 25).

Tg^{VE56} and Tg^{VE62} lines (of mixed background) were also bred to CD1 outbred $Gata2^{+/-}$ mice (2) to generate compound Tg^{VE}:$Gata2^{+/-}$ animals. Timed matings between Tg^{VE}:$GATA2^{+/-}$ and $Gata2^{+/fl}$ (10) animals were carried out. The morning of vaginal plug detection was defined as E0.5. Pregnant dams were gavaged daily with Tx (Sigma-Aldrich; 0.07 mg/g body weight) from E9 to E11. This dosage was experimentally determined to result in minimal embryonic lethality due to Tx toxicity (55). Embryos were isolated from Tx-treated pregnant dams on the gestational days described and were fixed in 4% paraformaldehyde and then digitally photographed as whole mounts, or gradually cleared in benzyl benzoate:benzyl alcohol before whole-mount photography. Alternatively, embryos were processed for paraffin embedding followed by H&E staining. Genomic DNAs of embryos isolated from yolk sacs were genotyped by PCR (Supplemental Table 1).

Flow cytometry. Embryos (E14.5) were harvested from Tx-treated pregnant dams. Yolk sacs were used for PCR genotyping. Individual FLs were isolated and triturated to generate single-cell suspensions. The cells were then filtered through cell strainers before being stained with unconjugated monoclonal antibodies (B220, CD3e, CD4, CD5, CD8a, Gr-1, and TER-119) that recognize mature hematopoietic lineages as well as directly conjugated antibodies (c-Kit, Sca-1, CD150, CD48), thus allowing the immunophenotyping of HSC-enriched fractions (56). Antibodies were purchased from Biolegend and eBioscience. Note that anti-Mac1 antibody was excluded from the lin^- cocktail, as FL HSCs are $Mac1^{lo}$ (57).

For ascertaining the effects of conditionally inactivating *Gata2* in the adult BM, 8- to 12-week-old mice (of mixed background) were gavaged with Tx (5 mg/day) for 5 consecutive days, and their BM cells were isolated for flow cytometric analyses 48 hours after the final Tx administration. BM cells were subjected to rbc lysis and then filtered through cell strainers, followed by magnetic depletion of mature hematopoietic lineage cells. The resultant lineage-negative (lin^-) cells were then stained with various antibodies prior to their staging by flow cytometry as described previously (58).

All flow studies were performed using a FACSAria (BD). The resulting cell distribution files were analyzed using FACSDiva (BD) or FlowJo (Tree Star Inc.) software. The statistical significance of differences between two groups of animals (as represented by the *P* value) was determined using Student's *t* test.

In vitro colony-forming assay. For methylcellulose colony-forming assays, single-cell suspensions were prepared from individual Tx-treated control and Tg^{VE}:*Gata2*$^{-/fl}$ E14.5 FLs. Unfractionated FL cells from individual embryos were seeded in triplicate in methylcellulose supplemented with various cytokines optimized to support the growth and differentiation of hematopoietic progenitors (M3434, Stem Cell Technologies). For control embryos, 2×10^4 total FL cells were seeded per plate. For Tg^{VE}:*Gata2*$^{-/fl}$ embryos, cells were seeded at multiple concentrations (2×10^4, 5×10^4, and 1×10^5 per plate) in triplicate. Colonies (comprising >30 cells) were scored as mixed (CFU-GEMM), myeloid (CFU-G, CFU-M, and CFU-GM), or erythroid (BFU-E) after 7–12 days of culture according to the manufacturer's instructions.

Competitive repopulation assay. Tg^{VE56} and Tg^{VE62} lines (of mixed background) were backcrossed to wild-type C57BL/6J mice for 5–6 generations and then bred to CD57BL/6-Ly5.2 *Gata2*$^{+/fl}$ mice to generate compound mutant Tg^{VE}:*Gata2*$^{+/fl}$ animals. Timed matings of Tg^{VE}:*Gata2*$^{+/fl}$ × *Gata2*$^{+/-}$ mice were initiated, and pregnant dams were gavaged daily from E9 to E11 with 0.07 mg/g body weight of Tx (Sigma-Aldrich). Embryos were harvested on gestational day 14.5 and kept in medium on ice while PCR genotyping was performed using yolk sac DNAs. After genotyping (~3 hours later), single-cell suspensions of FLs were prepared from the embryos of desired genotypes. CD57BL/6-Ly5.1 (B6-SJL, CD45.1) mice from 6 to 8 weeks of age were purchased from The Jackson Laboratory and were irradiated as previously described (58) for use as transplant recipients. CD45.2 FL cells (5×10^5) from control and test embryos were isolated from individual E14.5 embryos that had been exposed to Tx during development and were mixed at a 1:1 ratio with an equal number (5×10^5) of competitor CD45.1 adult BM cells. Cell mixtures were injected intravenously into lethally irradiated hosts. Donor chimerism in peripheral blood was determined by flow cytometry at 4, 8, 12, and 16 weeks after transplantation. Animals were considered positive for engraftment if more than 1% of tested cells were in the Gr-1$^+$Mac1$^+$ myeloid cell population. After 16 weeks, transplanted animals were sacrificed, and all of the BM cells recovered from 2 tibias and 2 femurs were processed for immunophenotyping of CD45.1 versus CD45.2 LSKS cells, as described above.

Statistics. Student's 1-tailed *t* test *P* values less than 0.05 in the pairwise comparisons were considered to be statistically significant.

Study approval. All animal experiments were carried out under a protocol approved by the University of Michigan IACUC (PRO00001725).

Acknowledgments

We gratefully acknowledge the helpful advice and assistance of, and spirited discussion with, members of our laboratory, as well as our colleagues Stephen J. Weiss, Sean Morrison, Jun-Lin Guan, and Ivan Maillard for critical evaluation of the manuscript. This work was supported initially by NIH grant R01 GM28896 and subsequently by the G. Carl Huber Professorship and NIH grant R01 AI94642 (to J.D. Engel).

Received for publication October 25, 2011, and accepted in revised form July 19, 2012.

Address correspondence to: James Douglas Engel, The University of Michigan Medical School, Cell and Developmental Biology, 109 Zina Pitcher Place, 3072 BSRB, Ann Arbor, Michigan 48109-2200, USA. Phone: 734.615.7509; Fax: 734.615.8500; E-mail: engel@umich.edu.

1. Yamamoto M, Ko LJ, Leonard MW, Beug H, Orkin SH, Engel JD. Activity and tissue-specific expression of the transcription factor NF-E1 multigene family. *Genes Dev*. 1990;4(10):1650–1662.
2. Tsai FY, et al. An early haematopoietic defect in mice lacking the transcription factor GATA-2. *Nature*. 1994;371(6494):221–226.
3. Zhou Y, et al. Rescue of the embryonic lethal hematopoietic defect reveals a critical role for GATA-2 in urogenital development. *EMBO J*. 1998; 17(22):6689–6700.
4. Khandekar M, Suzuki N, Lewton J, Yamamoto M, Engel JD. Multiple, distant Gata2 enhancers specify temporally and tissue-specific patterning in the developing urogenital system. *Mol Cell Biol*. 2004; 24(23):10263–10276.
5. Khandekar M, et al. A Gata2 intronic enhancer confers its pan-endothelia-specific regulation. *Development*. 2007;134(9):1703–1712.
6. Zhou Y, Yamamoto M, Engel JD. GATA2 is required for the generation of V2 interneurons. *Development*. 2000;127(17):3829–3838.
7. Minegishi N, et al. Expression and domain-specific function of GATA-2 during differentiation of the hematopoietic precursor cells in midgestation mouse embryos. *Blood*. 2003;102(3):896–905.
8. Craven SE, Lim KC, Ye W, Engel JD, de Sauvage F, Rosenthal A. Gata2 specifies serotonergic neurons downstream of sonic hedgehog. *Development*. 2004; 131(5):1165–1173.
9. Hoshino T, et al. Reduced BMP4 abundance in Gata2 hypomorphic mutant mice result in uropathies resembling human CAKUT. *Genes Cells*. 2008; 13(2):159–170.
10. Charles MA, et al. Pituitary-specific Gata2 knockout: effects on gonadotrope and thyrotrope function. *Mol Endocrinol*. 2006;20(6):1366–1377.
11. Willett RT, Greene LA. Gata2 is required for migration and differentiation of retinorecipient neurons in the superior colliculus. *J Neurosci*. 2011; 31(12):4444–4455.
12. Tsai FY, Orkin SH. Transcription factor GATA-2 is required for proliferation/survival of early hematopoietic cells and mast cell formation, but not for erythroid and myeloid terminal differentiation. *Blood*. 1997;89(10):3636–3643.
13. Ling KW, et al. GATA-2 plays two functionally distinct roles during the ontogeny of hematopoietic stem cells. *J Exp Med*. 2004;200(7):871–882.
14. Rodrigues NP, et al. Haploinsufficiency of GATA-2 perturbs adult hematopoietic stem-cell homeostasis. *Blood*. 2005;106(2):477–484.
15. Feil R, Wagner J, Metzger D, Chambon P. Regulation of Cre recombinase activity by mutated estrogen receptor ligand-binding domains. *Biochem Biophys Res Commun*. 1997;237(3):752–757.
16. Ostergaard P, et al. Mutations in GATA2 cause primary lymphedema associated with a predisposition to acute myeloid leukemia (Emberger syndrome). *Nat Genet*. 2011;43(10):929–931.
17. Kazenwadel J, et al. Loss-of-function germline GATA2 mutations in patients with MDS/AML or MonoMAC syndrome and primary lymphedema reveal a key role for GATA2 in the lymphatic vasculature. *Blood*. 2012;119(5):1283–1291.
18. Ishida H, et al. GATA-2 anomaly and clinical phenotype of a sporadic case of lymphedema, dendritic cell, monocyte, B- and NK-cell (DCML) deficiency, and myelodysplasia. *Eur J Pediatr*. 2012;171(8):1273–1276.
19. Shaner NC, Campbell RE, Steinbach PA, Giepmans BN, Palmer AE, Tsien RY. Improved monomeric red, orange and yellow fluorescent proteins derived from Discosoma sp. red fluorescent protein. *Nat Biotechnol*. 2004;22(12):1567–1572.
20. Brandt W, Khandekar M, Suzuki N, Yamamoto M, Lim KC, Engel JD. Defining the functional boundaries of the Gata2 locus by rescue with a linked bacterial artificial chromosome transgene. *J Biol Chem*. 2008;283(14):8976–8983.
21. Suzuki N, et al. Combinatorial Gata2 and Sca1 expression defines hematopoietic stem cells in the bone marrow niche. *Proc Natl Acad Sci U S A*. 2006; 103(7):2202–2207.
22. Minegishi N, et al. The mouse GATA-2 gene is expressed in the para-aortic splanchnopleura and aorta-gonads and mesonephros region. *Blood*. 1999;93(12):4196–4207.
23. Nozawa D, Suzuki N, Kobayashi-Osaki M, Pan X, Engel JD, Yamamoto M. GATA2-dependent and region-specific regulation of Gata2 transcription in the mouse midbrain. *Genes Cells*. 2009;14(5):569–582.
24. Motoike T, et al. Universal GFP reporter for the study of vascular development. *Genesis*. 2000;28(2):75–81.
25. Soriano P. Generalized lacZ expression with the ROSA26 Cre reporter strain. *Nat Genet*. 1999; 21(1):70–71.
26. Srinivasan RS, et al. Lineage tracing demonstrates the venous origin of the mammalian lymphatic vasculature. *Genes Dev*. 2007;21(19):2422–2432.
27. Francois M, Harvey NL, Hogan BM. The transcriptional control of lymphatic vascular development. *Physiology*. 2011;26(3):146–155.
28. North TE, et al. Runx1 expression marks long-term repopulating hematopoietic stem cells in the midgestation mouse embryo. *Immunity*. 2002;16(5):661–672.
29. Yokomizo T, Ng CE, Osato M, Dzierzak E. Three-dimensional imaging of whole midgestation murine embryos shows an intravascular localization for all hematopoietic clusters. *Blood*. 2011; 117(23):6132–6134.
30. Zovein AC, et al. Fate tracing reveals the endothelial origin of hematopoietic stem cells. *Cell Stem Cell*. 2008;3(6):625–636.
31. Grass JA, et al. Distinct functions of dispersed GATA factor complexes at an endogenous gene locus. *Mol Cell Biol*. 2006;26(19):7056–7067.
32. Kiel MJ, Yilmaz OH, Iwashita T, Terhorst C, Morrison SJ. SLAM family receptors distinguish hematopoietic stem and progenitor cells and reveal endothelial niches for stem cells. *Cell*. 2005;121(7):1109–1121.
33. Kim I, He S, Yilmaz OH, Kiel MJ, Morrison SJ. Enhanced purification of fetal liver hematopoietic stem cells using SLAM family receptors. *Blood*. 2006;108(2):737–744.
34. He S, Kim I, Lim MS, Morrison SJ. Sox17 expression confers self-renewal potential and fetal stem

cell characteristics upon adult hematopoietic progenitors. *Genes Dev*. 2011;25(15):1613–1627.
35. Kaneko H, Shimizu R, Yamamoto M. GATA factor switching during erythroid differentiation. *Curr Opin Hematol*. 2010;17(3):163–168.
36. Rodrigues NP, et al. GATA-2 regulates granulocyte-macrophage progenitor cell function. *Blood*. 2008;112(13):4862–4873.
37. Kobayashi-Osaki M, et al. GATA motifs regulate early hematopoietic lineage-specific expression of the Gata2 gene. *Mol Cell Biol*. 2005;25(16):7005–7020.
38. Medvinsky A, Dzierzak E. Definitive hematopoiesis is autonomously initiated by the AGM region. *Cell*. 1996;86(6):897–906.
39. Snow JW, et al. Context-dependent function of "GATA switch" sites in vivo. *Blood*. 2011;117(18):4769–4772.
40. Bresnick EH, Lee HY, Fujiwara T, Johnson KD, Keles S. GATA switches as developmental drivers. *J Biol Chem*. 2010;285(41):31087–31093.
41. Snow JW, et al. A single cis element maintains repression of the key developmental regulator Gata2. *PLoS Genet*.2010;6(9):e1001103.
42. Challen GA, Boles NC, Chambers SM, Goodell MA. Distinct hematopoietic stem cell subtypes are differentially regulated by TGF-beta1. *Cell Stem Cell*. 2010;6(3):265–278.
43. Wilson A, et al. Hematopoietic stem cells reversibly switch from dormancy to self-renewal during homeostasis and repair. *Cell*. 2008;135(6):1118–1129.
44. Weksberg DC, Chambers SM, Boles NC, Goodell MA. CD150- side population cells represent a functionally distinct population of long-term hematopoietic stem cells. *Blood*. 2008;111(4):2444–2451.
45. Lugus JJ, et al. GATA2 functions at multiple steps in hemangioblast development and differentiation. *Development*. 2007;134(2):393–405.
46. Schulte-Merker S, Sabine A, Petrova TV. Lymphatic vascular morphogenesis in development, physiology, and disease. *J Cell Biol*. 2011;193(4):607–618.
47. Uhrin P, et al. Novel function for blood platelets and podoplanin in developmental separation of blood and lymphatic circulation. *Blood*. 2010; 115(19):3997–4005.
48. Carramolino L, Fuentes J, Garcia-Andres C, Azcoitia V, Riethmacher D, Torres M. Platelets play an essential role in separating the blood and lymphatic vasculatures during embryonic angiogenesis. *Circ Res*. 2010;106(7):1197–1201.
49. Sebzda E, et al. Syk and Slp-76 mutant mice reveal a cell-autonomous hematopoietic cell contribution to vascular development. *Dev Cell*. 2006;11(3):349–361.
50. Abtahian F, et al. Regulation of blood and lymphatic vascular separation by signaling proteins SLP-76 and Syk. *Science*. 2003;299(5604):247–251.
51. Ichise H, Ichise T, Ohtani O, Yoshida N. Phospholipase Cgamma2 is necessary for separation of blood and lymphatic vasculature in mice. *Development*. 2009;136(2):191–195.
52. Feil R, Walter J, Allen ND, Reik W. Developmental control of allelic methylation in the imprinted mouse Igf2 and H19 genes. *Development*. 1994; 120(10):2933–2943.
53. Chung JH, Whiteley M, Felsenfeld G. A 5′ element of the chicken β-globin domain serves as an insulator in human erythroid cells and protects against position effects in Drosophila. *Cell*. 1993;74(3):505–514.
54. Moriguchi T, et al. Gata3 participates in a complex transcriptional feedback network to regulate sympathoadrenal differentiation. *Development*. 2006;133(19):3871–3881.
55. Park EJ, Sun X, Nichol P, Saijoh Y, Martin JF, Moon AM. System for tamoxifen-inducible expression of cre-recombinase from the Foxa2 locus in mice. *Dev Dyn*. 2008;237(2):447–453.
56. Hosoya T, et al. GATA-3 is required for early T lineage progenitor development. *J Exp Med*. 2009; 206(13):2987–3000.
57. Morrison SJ, Hemmati HD, Wandycz AM, Weissman IL. The purification and characterization of fetal liver hematopoietic stem cells. *Proc Natl Acad Sci U S A*. 1995;92(22):10302–10306.
58. Ku CJ, Hosoya T, Maillard I, Engel JD. GATA-3 regulates hematopoietic stem cell maintenance and cell-cycle entry. *Blood*. 2012;119(10):2242–2251.